A Case Study loosely based on the Stanford University Campus Airside and Waterside HVAC Systems

Abstract

We present a large-scale industrially relevant case study where solving a single MPC optimization problem is not feasible for real-time implementations. The study is loosely based on the Stanford University campus, consisting of both an airside and waterside system. The airside system includes 500 zones spread throughout 25 campus buildings along with the air handler units and regulatory building automation system used for temperature regulation. The waterside system includes the central plant equipment, such as chillers, that is used to meet the load from the buildings. Active thermal energy storage is also available to the campus. The models from this case study are made publicly available for other researchers interested in designing alternative control strategies for managing chilled water production to meet airside loads. The aim of the case study release is to provide a standardized problem for the research community and a benchmark for evaluating performance.

1 CASE STUDY

1.1 Background

The case study is modeled after the Stanford University campus (Rawlings et al., 2018). Recently, Stanford University replaced an aging natural gas cogeneration plant with a new heat-recovery system to meet the cooling and heating loads of their campus as part of the $485-million Stanford Energy System Innovations (SESI) project (Blair, 2016). In addition to adding heat-recovery chillers to improve efficiency, thermal energy storage tanks were added for hot and chilled water. These large insulated tanks, along with the rest of the central HVAC plant, are depicted in Figure 1. Johnson Controls designed the control architecture for the new central plant. Results have shown that the MPC-based system achieves 10–15% more energy cost savings compared to the best team of trained human operators (Stagner, 2016). While this project was focused primarily on optimization of the waterside, the case study is being extended to include treatment of the airside system as well.

Certain aspects of this real-world problem have inspired research projects for creating economically optimal methods of controlling such a large-scale industrial system. For the case study presented in this paper, a simplified version of the Stanford project is used to highlight the complexity of controlling a large-scale combined airside and waterside system while removing some of the problem features and intricate details to increase clarity for a research perspective.

1.2 System

The HVAC system for the case study is a central plant that services the cooling needs of a 500-zone campus. The HVAC plant has eight conventional chillers along with their supporting pumps and cooling towers. For simplicity, we do not consider heating equipment, such as boilers or heat-recovery chillers. Each of the chillers has minimum and maximum cooling capacities of 2.5 MW and 12.5 MW, yielding a total plant capacity of 100 MW cooling. Chilled water supply temperature is held constant at 5.5 °C. In addition to the passive thermal energy storage present in the form of building mass, there is active thermal energy storage with a chilled water tank. The chilled water TES storage tank has a maximum capacity of 100 MWh cooling.

The 500-zone campus contains 25 buildings, each with 20 zones that have independent local temperature controllers. All zone temperatures need to be kept between 20.5 and 22.5 °C to ensure occupant comfort. The models for the equipment and zones are presented in Section 2. The airside models describe the temperature

Figure 1: The new heat-recovery system to provide heating and cooling to the campus constructed as part of the $485-million Stanford Energy System Innovations (SESI) project Blair (2016).

Table 1: Parameters

Variable	Description	Data Field	Unit
t	Time	`param.time`	h
T_a	Ambient Temperature	`param.AmbientTemp`	℃
c_k	Electricity Pricing	`param.ElecPrices`	US$
c_{peak}	Monthly Demand Charge	`param.DemandCharge`	US$
T_{min}	Lower Bound of Comfort Zone	`param.ComfortMin`	℃
T_{max}	Upper Bound of Comfort Zone	`param.ComfortMax`	℃
s_{max}	Active TES Capacity	`param.StorageCapacity`	kWh

dynamics in each of the 500 zones, and the waterside models describe the power consumption of the central plant equipment.

The aim of the control system is to minimize costs in the presence of time-varying electricity prices and a peak demand charge as well as environmental disturbances such as weather while meeting constraints on comfort and equipment. The control system must determine the zone temperature setpoints and waterside equipment operation schedule.

1.3 Parameters

Several loads are placed on the HVAC system. The primary disturbance considered in this study is the ambient temperature. Typical ambient temperature data during the summer for a city in the Southern U.S. is presented in Figure 2. To reject the loads placed on the campus, the HVAC system purchases power from the electricity market. Two components of the pricing structure are considered in this study: time-of-use charges, which assess time-varying prices on electricity use throughout the day, and peak demand charges, which are proportional to maximum rate of power consumption over period of time (typically a month). Electricity pricing data obtained from Johnson Controls over a week-long period is given in Figure 2. The monthly peak demand charge is $4.56/kW. The parameters for this case study are provided in the associated data file and are summarized in Table 1.

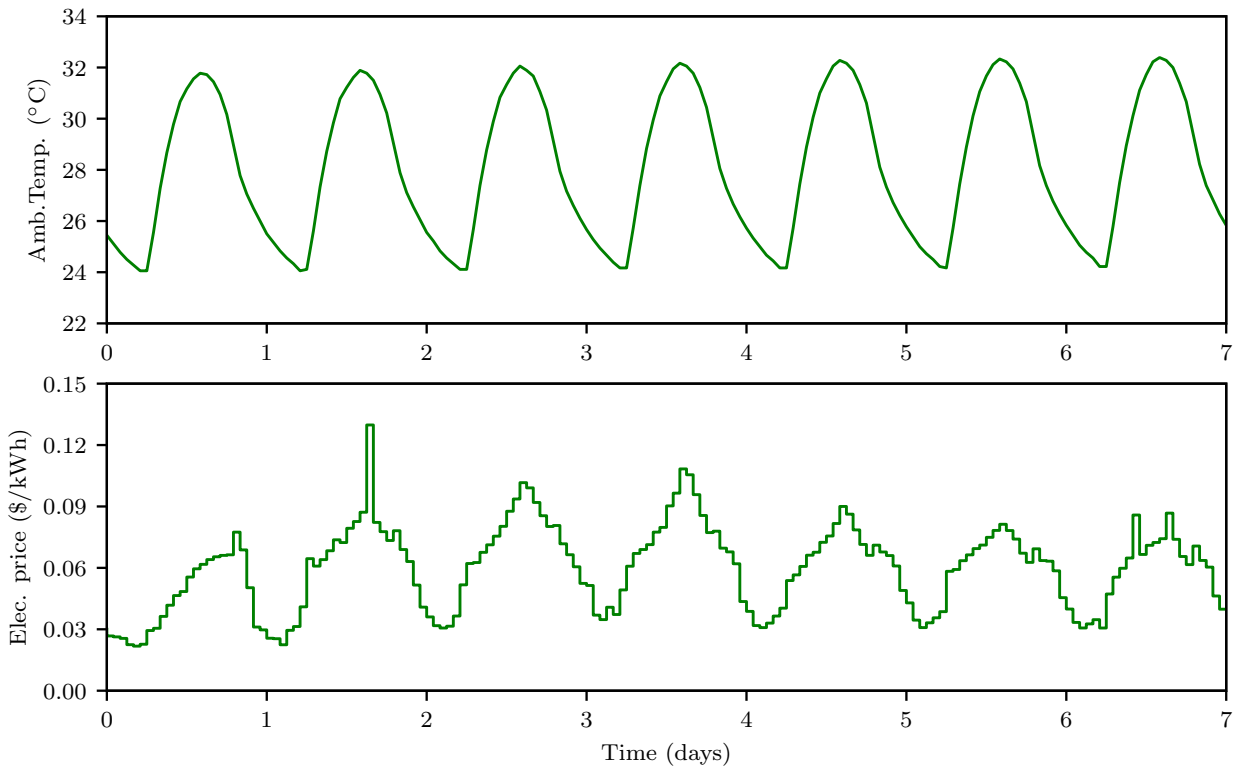

Figure 2: Representative ambient temperature and electricity pricing data over a 7-day period in the summer (Rawlings et al., 2018). In this plot, zero corresponds to midnight.

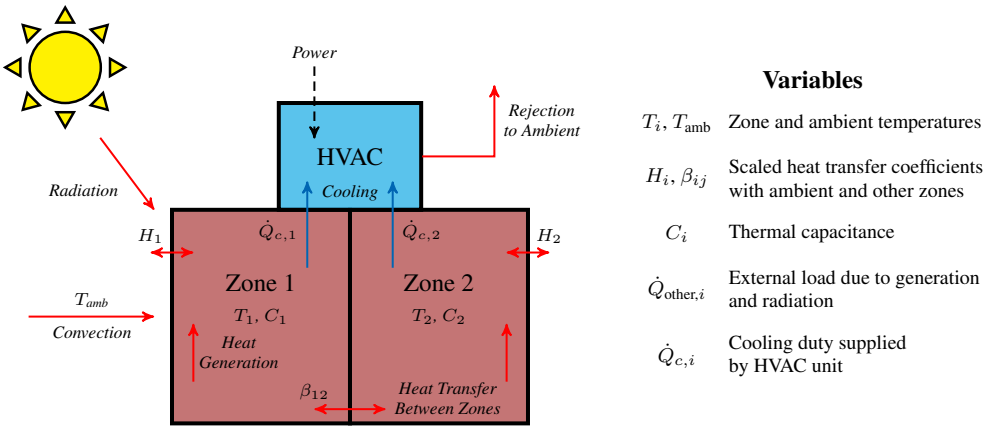

Figure 3: Diagram of airside heat transfer.

Table 2: Airside Model Parameters

Variable	Description	Data Field	Unit
H_i	Scaled Heat Transfer Coefficient with Ambient	`airside.H`	kW/K
C_i	Thermal Capacitance	`airside.C`	kJ/K
β_{ij}	Scaled Heat Transfer Coefficient between Zones	`airside.Beta`	kW/K
$\dot{Q}_{\mathrm{ss},i}$	PI Steady State Cooling	`airside.Qss`	kW
$K_{\mathrm{c},i}$	PI Controller Gain	`airside.Kc`	kW/K
$\tau_{\mathrm{I},i}$	PI Integral Time Constant	`airside.tauI`	h

2 MODELS

2.1 Airside System

In the airside system, models are needed to describe temperature dynamics. The dynamics of cooling a single zone or building can be represented by an energy balance. For simplicity, we considered the lumped model for the temperature of zone i as given by

$$C_i \frac{dT_i}{dt} = -H_i(T_i - T_a) - \sum_{j \neq i} \beta_{ij}(T_i - T_j) - \dot{Q}_{c,i} + \dot{Q}_{\mathrm{other},i} \tag{1}$$

in which C_i is the thermal capacitance of the zone, H_i is a scaled heat transfer coefficient with the ambient, T_a is the ambient temperature, $\dot{Q}_{c,i}$ is the cooling rate from the HVAC system, $\dot{Q}_{\mathrm{other},i}$ is an external load place on the zone, and β_{ij} characterizes the degree of coupling between zones i and j. If zones i and j are not adjacent, then $\beta_{ij} = 0$. The heat transfer is depicted in Figure 3

Since the supervisory control system determines the zone temperature setpoints, a model is also need to relate the zone temperature setpoint $T_{\mathrm{sp},i}$ to the cooling rate $\dot{Q}_{c,i}$ delivered to the zone. Using an ideal proportional-integral (PI) controller, the linear cooling duty controller model is given by

$$\begin{aligned} \dot{Q}_{c,i} &= \dot{Q}_{\mathrm{ss},i} + K_{\mathrm{c},i}\left[\varepsilon_i + \frac{1}{\tau_{\mathrm{I},i}}\int_0^t \varepsilon_i(t')dt'\right] \\ \varepsilon_i &= T_{\mathrm{sp},i} - T_i \end{aligned} \tag{2}$$

in which $K_{\mathrm{c},i}$ and $\tau_{\mathrm{I},i}$ are the PI controller parameters and ε_i is the tracking error. The airside model parameters for this case study are provided in the associated data file and are summarized in Table 2. In the data file, these airside parameters are grouped by building and presented as a cell array of length of 25 with each cell containing the parameter values for the 20 zones in that particular building.

2.2 Waterside System

In the waterside system, models are needed for equipment electricity consumption and storage tank dynamics. Equipment models are static, determining resource consumption as a function of relevant inputs for a given steady-state operating point. While these units do experience transient dynamics during startup and shutdown, these effects are moderated by local regulatory controllers, and rapid startups and shutdowns are prevented by enforcing explicit dwell time constraints in the waterside optimization problem. By contrast, storage tank models are necessarily dynamic, as storage tanks are used for time-shifting of demand. We assume throughout that the enthalpy H of a volume V of water at uniform temperature T is given by

$$H = \rho C_p V (T - T_{\text{ref}}) \tag{3}$$

in which ρ is the (constant) density, C_p is the (constant) heat capacity, and T_0 is an arbitrary reference temperature.

For the chilling plant used in the case study, the three types of equipment are chillers, cooling towers, and pumps. Figure 4 shows the mass and energy flows for this system. Note that the real system consists of multiple pieces of each type of equipment arranged in parallel. Each chiller is modeled using the semi-empirical Gordon-Ng model, Lee et al. (2012) defined below:

$$W_{\text{CH}} \coloneqq \left(Q_{\text{CH}} + a_1 T_{\text{CHWS}} + a_2 \left(1 - \frac{T_{\text{CHWS}}}{T_{\text{CWS}}} \right) \right) \frac{T_{\text{CWS}}}{T_{\text{CHWS}} - a_3 Q_{\text{CH}}} - Q_{\text{CH}} \tag{4}$$

The parameters a_1, a_2, and a_3 are obtained via regression with measured data. For the purposes of optimization, the temperatures are assumed to be fixed parameters. The required volumetric flow is then calculated from the enthalpy relationship (3). Each cooling tower uses a a simplified effectiveness model Jin et al. (2007) for calculating cooling duty, with a simple cubic fit for fan electricity Braun and Diderrich (1990).

$$Q_{\text{CT}} = Q_{\text{CH}} + Q_{\text{CH}} \coloneqq \frac{c_1 (m_{\text{CW}})^{c_3}}{1 + c_2 \left(\frac{m_{\text{CW}}}{m_{\text{air}}} \right)^{c_3}} (T_{\text{CWR}} - T_{\text{WB}}) \tag{5}$$

$$W_{\text{CT}} \coloneqq \kappa (m_{\text{air}})^3 \tag{6}$$

With fixed T_{CWR} and T_{CWS}, the required water flow rate m_{CW} can be calculated from an enthalpy balance. Then, using the known T_{WB}, (5) can be rearranged to solve for the required m_{air}, which is then used in (6) for electricity calculation. Coefficients c_1, c_2, c_3, and κ are obtained via regression. Finally, pumps are modeled with a black-box empirical model

$$W_{\text{P}} \coloneqq b_1 \ln (1 + b_2 V_{\text{CHW}}) + b_3 V_{\text{CHW}} + b_4 \tag{7}$$

with regression coefficients b_1 through b_4. Note that the flows V_{CW} and m_{CW} are obtained from Q_{CH} and Q_{CT} via the appropriate constant-heat-capacity energy balances.

Active storage tanks are modeled using a two-layer stratified tank model similar to Ma et al. (2012). As diagrammed in Figure 5, the hot and cold sections are each assumed to be uniform in temperature, with heat exchange between the two layers (proportional to the temperature difference). The tank is well-insulated, but heat exchange (proportional to the temperature difference) takes place between the two layers. With state vector $(V_{\text{cold}}, V_{\text{hot}}, H_{\text{cold}}, H_{\text{hot}})$, the differential equations are as follows:

$$\begin{aligned}
\frac{dV_{\text{hot}}}{dt} &= -v_+ + v_-, \\
\frac{dV_{\text{cold}}}{dt} &= v_+ - v_-, \\
\frac{dH_{\text{hot}}}{dt} &= -\frac{H_{\text{hot}}}{V_{\text{hot}}} v_+ + h_- v_- - K \left(\frac{H_{\text{hot}}}{V_{\text{hot}}} - \frac{H_{\text{cold}}}{V_{\text{cold}}} \right), \\
\frac{dH_{\text{cold}}}{dt} &= h_+ v_+ - \frac{H_{\text{cold}}}{V_{\text{cold}}} v_- + K \left(\frac{H_{\text{hot}}}{V_{\text{hot}}} - \frac{H_{\text{cold}}}{V_{\text{cold}}} \right),
\end{aligned}$$

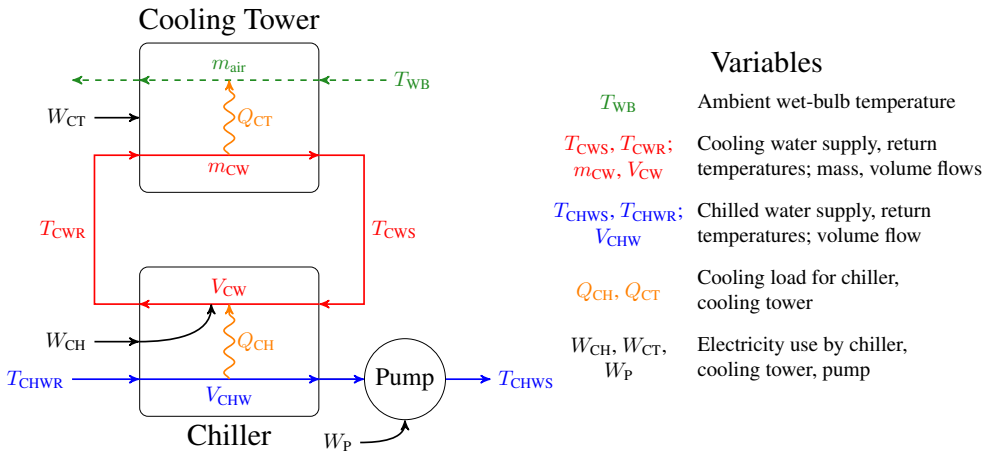

Figure 4: Diagram of a single chiller, cooling tower, and pump.

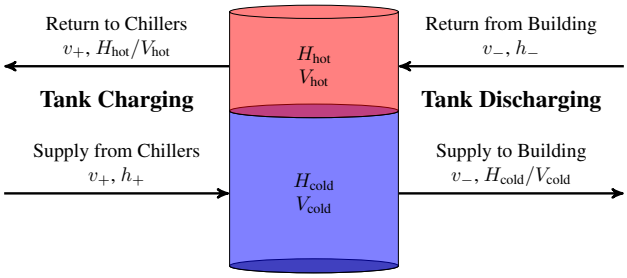

Figure 5: Diagram of stratified tank model.

in which inputs v_+ and v_- are the charge and discharge volumetric flows, and parameters h_+ and h_- are the (per-volume) supply and return enthalpies, with heat transfer coefficient K between the two layers. The corresponding temperatures T_{hot} and T_{cold} are calculated from the linear enthalpy relationship (3), as are the volumetric enthalpies h_+ and h_- of the incoming streams. In chilled water tanks, the state of interest is the enthalpy of the cold section H_{cold}, while for hot water tanks, it is H_{hot}. Total volume $V_{\text{hot}} + V_{\text{cold}} = V_{\text{total}}$ is held constant.

For the purposes of optimization, the nonlinear tank model is replaced by a simple linear approximation of the form

$$\frac{ds}{dt} = -\sigma s + \eta \dot{Q}_{\text{storage}} \tag{8}$$

in which $s := H_{\text{cold}}$ is the enthalpy of the cold section and $\dot{Q}_{\text{storage}}$ is the rate of cold enthalpy inflow (positive) or outflow (negative). The coefficients σ and η are identified from data.

All waterside parameters are shown in Table 3, with numerical values given in the data file.

2.3 Availability

The full set of data and model parameters for the case study are made publicly available for researchers in the HVAC community. They can be found on the following website: `https://hvacstudy.github.io/`. The aim of the release is to encourage other researchers to propose alternative control systems and to provide a common basis for performance evaluation of these strategies on a large-scale industrially relevant system.

Table 3: Waterside Model Parameters

Variable	Description	Data Field	Unit
T_{CHWS}	Constant chilled water supply temperature	`waterside.common.Tchws`	°C
T_{CHWR}	Constant chilled water return temperature	`waterside.common.Tchwr`	°C
T_{CWS}	Constant chilled water supply temperature	`waterside.common.Tchwr`	°C
ρ	Water density	`waterside.common.rho`	kg/m^3
C_p	Water heat capacity	`waterside.common.Cp`	kJ/(kg °C)
T_{ref}	Enthalpy reference temperature	`waterside.common.Tref`	°C
$Q_{\text{CH}}^{\min}$	Minimum chiller cooling duty	`waterside.chiller.Qmin`	kW
$Q_{\text{CH}}^{\max}$	Maximum chiller cooling duty	`waterside.chiller.Qmax`	kW
a_i	Chiller regression coefficients	`waterside.chiller.a`	varies
$Q_{\text{CT}}^{\min}$	Minimum cooling tower duty	`waterside.tower.Qmin`	kW
$Q_{\text{CT}}^{\max}$	Maximum cooling tower duty	`waterside.tower.Qmax`	kW
c_i	Cooling tower regression coefficients	`waterside.tower.c`	varies
κ	Cooling tower fan coefficient	`waterside.tower.kappa`	kJ/kg
$V^{\min}$	Minimum pump flow rate	`waterside.pump.Vmin`	m^3/s
$V^{\max}$	Maximum pump flow rate	`waterside.pump.Vmax`	m^3/s
b_i	Pump regression parameters	`waterside.pump.b`	varies
V_{total}	Total tank volume	`waterside.tank.Vtot`	m^3
K	Layer heat transfer coefficient	`waterside.tank.K`	m^3

References

Blair, S. (2016). Editors' choice and best energy/industrial: Stanford Energy System Innovations. *Engineering News-Record*. Retrieved from `http://www.enr.com/articles/39005-editors-choice-best-energyindustrial-stanford-energy-system-innovations`.

Braun, J. E. and Diderrich, G. T. (1990). Near-optimal control of cooling towers for chilled-water systems. *ASHRAE Transactions*, 96(CONF-9006117).

Jin, G.-Y., Cai, W.-J., Lu, L., Lee, E. L., and Chiang, A. (2007). A simplified modeling of mechanical cooling tower for control and optimization of HVAC systems. *Energ. Convers. Manage.*, 48(2):355–365.

Lee, T.-S., Liao, K.-Y., and Lu, W.-C. (2012). Evaluation of the suitability of empirically-based models for predicting energy performance of centrifugal water chillers with variable chilled water flow. *Appl. Energ.*, 93(0):583–595.

Ma, Y., Borrelli, F., Hencey, B., Coffey, B., Bengea, S., and Haves, P. (2012). Model predictive control for the operation of building cooling systems. *IEEE Ctl. Sys. Tech.*, 20(3):796–803.

Rawlings, J. B., Patel, N. R., Risbeck, M. J., Maravelias, C. T., Wenzel, M. J., and Turney, R. D. (2018). Economic MPC and real-time decision making with application to large-scale HVAC energy systems. *Comput. Chem. Eng.*, 114:89–98. FOCAPO/CPC 2017.

Stagner, J. (2016). Enterprise optimization solution (EOS) cost savings vs. manual plant dispatching. Report on Central Energy Facility, Stanford Energy System Innovations.

Acknowledgment

The authors gratefully acknowledge the financial support of the NSF through grant #CTS-1603768 as well as Johnson Controls, Inc. for providing sample data, models, and research funding.